fermentation

MDPI

Article

Dichlororesorcinols Produced by a Rhizospheric Fungi of *Panax notoginseng* as Potential ERK2 Inhibitors

Yingying Wu [1,†], Mengyue Zhang [1,†], Jinyan Xue [1], Juan Cheng [1], Mingyu Xia [1], Xunyong Zhou [2] and Yixuan Zhang [1,*]

[1] Department of biopharmaceutical Sciences, School of Life Science and Biopharmaceutics, Shenyang Pharmaceutical University, Shenyang 110016, China; wyy280884549@163.com (Y.W.)
[2] Zhen Cui (Jiangsu) Enzyme Biology Ltd., Suqian 223800, China; zimmernchow@126.com
* Correspondence: zhangyxzsh@163.com; Tel.: +86-24-43520921; Fax: +86-24-23986401
† These authors contributed equally to this work.

Abstract: Rhizospheric fungi of medicinal plants are important sources for discovering novel and valuable secondary metabolites with potential pharmaceutical applications. In our research, five new dichlororesorcinols (**1–5**) and five known metabolites (**6–10**) were separated from the secondary metabolites of *Chaetomium* sp. SYP-F6997, which was isolated from the rhizospheric soil of *Panax notoginseng*. The identification of these compounds was confirmed using various spectroscopic techniques including ESI-MS, UV, IR, NMR and ECD analyses. These findings highlight the potential of rhizospheric fungi as a rich source of novel bioactive compounds. In addition, chiral HPLC was used to successfully separate the enantiomers compound **4** and compound **5**, and TDDFT-ECD/optical rotation calculations were used to test their absolute configurations. This is the first report of compounds **1–10** from the genus *Chaetomium*, and the first report of compounds **1–5** and **7** from the family *Chaetomiaceae*. We proposed plausible biosynthetic pathways for dichlororesorcinols **1–6** based on their analogous carbon skeleton. These findings provide insights into the biosynthesis of these compounds and expand our understanding of the secondary metabolites produced by *Chaetomium* sp. SYP-F6997. To evaluate their potential as therapeutic agents, we investigated the cytotoxic activity of all the isolated metabolites against cell lines H9, HL-60, K562, THP-1 and CEM using the MTT method. The new compounds **1** and **2** exhibited significant cytotoxic activities against H9 and CEM, with IC50 values lower than 10 μM. To further explore the potential mechanisms of action, we performed molecular docking studies to investigate the interactions between compounds **1** and **2** with the potential target ERK2. Our results demonstrate that the compounds exhibited strong binding abilities and formed H-bond interactions with ERK2, providing support for their potent antitumor activities and promising potential as lead molecules for the development of antitumor therapeutics.

Keywords: rhizospheric fungi; *Chaetomium* sp.; dichlororesorcinols; antitumor activity

Citation: Wu, Y.; Zhang, M.; Xue, J.; Cheng, J.; Xia, M.; Zhou, X.; Zhang, Y. Dichlororesorcinols Produced by a Rhizospheric Fungi of *Panax notoginseng* as Potential ERK2 Inhibitors. *Fermentation* **2023**, *9*, 517. https://doi.org/10.3390/fermentation9060517

Academic Editor: Mónica Gandía

Received: 31 March 2023
Revised: 20 May 2023
Accepted: 24 May 2023
Published: 27 May 2023

1. Introduction

Panax notoginseng F. H. Chen (Araliaceae) has been an important herbal drug for centuries in Asia [1]. It has been widely used for its antidiabetic, antioxidant and antitumor biological activities [2,3]. Medicinal plants usually harbor endophytic or rhizospheric fungi which are regarded as sources of important pharmaceutical products [4–7]. Considering the symbiosis between the host plant *P. notoginseng* and its related endophytic or rhizospheric fungi, we conducted research to discover novel substances with anti-cancer or antimicrobial abilities through microbial fermentation [5,8,9].

ERKs are members of protein serine/threonine kinases. ERKs play a mediating and amplifying role in tumor invasion and metastasis [10]. They are key targets belonging to the mitogen-activated family. ERK1 and ERK2 are subtypes of ERKs, and they have been studied in many malignant tumors such as breast, lung, bladder and ovarian cancer [11,12].

ERK1 and ERK2 are components of the Ras/Raf/MEK/ERK pathway and they are involved in triggering many cellular reactions in the cancer process [13]. There have been various inhibitors of ERK1/2 reported in the past several decades [11,12,14]. However, most of them are still in clinical trials without FDA approval. The numbers of ERK1/2 inhibitors currently in clinical trials is still less than those targeting other pathways [14]. Due to the clinical significance of ERK1/2 inhibitors, they are continuously explored in resistant tumor cell lines by researchers. The inhibition of ERKs can restrain cell proliferation, differentiation and survival [15,16]. Therefore, compounds that can bind to ERKs might be candidates for potent ERK inhibitors. Despite an 84% sequence similarity between ERK1 and ERK2, ERK2 plays a key role in driving cell proliferation [17–19]. Thus, a molecular docking approach was used to explore the probable mechanism between the active substances and ERK2 in this study. Secondary metabolites with novel structures and significant biological activities from endophytic fungi have always been research hotspots [20–22].

In this study, five new dichlororesorcinol compounds (**1–5**) and five known compounds (**6–10**) were isolated and identified from microbial fermentation of *Chaetomium* sp. All the substances (**1–10**) were tested for cytotoxicity. Further, a molecular docking analysis was carried out for mechanism investigation.

2. Materials and Methods

2.1. General Experimental Procedures

The UV and optical rotation data were obtained using a P-2000 digital polarimeter (JASCO, Kyoto, Japan). A MOS-450 spectrometer (Bio-Logic Science, Claix, France) was used to record the circular dichroism (CD) spectrum. Bruker NMR spectrometers (Rheinstetten, Bremen, Germany) were used for ^{1}H (400 MHz), ^{13}C (100 MHz) and 2D NMR spectra. A Bruker Customer TOF-Q mass spectrometer (MA, Daltonics, Germany) was used to measure the mass spectra (HR-ESI-MS). CH_3CN, MeOH, n-Hexane and isopropyl alcohol of chromatographic grade (Merck, Darmstadt, Germany) were used for HPLC analysis. All solvents used were bought from Tianjin Kemiou Chemical Reagent Company (Tianjing, China). Silica gel, including 100–200 mesh and 200–300 mesh, was bought from Qingdao Marine Chemical Factory (Qingdao, China). Semi-preparative and RP-HPLC isolations were performed using a Shimadzu LC-20AB instrument equipped with a YMC C18 column (10 mm × 250 mm, 5 μm) and an SPD-20A detector. Chiral HPLC separation was achieved with a column of CHIRALCEL-OJ-H (4.6 mm × 250 mm, 5 μm) equipped with a Shimadzu LC-20AB facility using a Shimadzu SPD-10A UV detector.

2.2. Fungal Material and Fermentation

The fungal strain in this research was isolated from the rhizospheric soil of *Panax notoginseng*, collected from Wenshan, Yunnan, China, and identified based on the DNA sequence (ITSI-5.8S-ITS2-28S), which has been submitted to GenBank with accession number OQ945315. The BLAST search result revealed that the isolate had the highest identity (99.24%) with the species Chaetomium udagawae. The colony morphology characteristics on a PDA medium are shown in Figure S1A,B. The microstructure was observed under an optical microscope, as shown in Figure S1C,D. A mixture of water and rice at a ratio of 55 mL/40 g was added to a conical flask (250 mL) and sterilized for 30 min at 121 °C. The spores of *Chaetomium* sp. were then added. One hundred and twenty solid fermentation flasks were incubated for 30 days at a temperature of 26 °C. The fermentation mixture was then crushed and extracted with ethyl acetate (30 L) overnight. This operation was repeated four times to obtain crude substances (110 g).

2.3. Isolation of Secondary Metabolites

The crude substances (110 g) were dissolved in 90% MeOH–H_2O (500 mL), and the mixture was extracted with hexane (500 mL) three times to obtain a residue (70 g). Two silica gel columns with pore diameters of 100–200 mesh and 200–300 mesh were used to separate

the extract (70 g) by column chromatography (CC). Petroleum ether-EtOAc was used as the eluent with a gradient from 80:1 to 3:1.

As results, six fractions (A–F) were obtained. The ODS in gradient from MeOH–H_2O 10:90 to 90:10 was used for isolating Fraction B (22.9 g), and eight fractions (B1–B8) were obtained. Fraction B3 (1.8 g) was added to a preparative HPLC (MeOH–H_2O, 70%) as an eluent, yielding substances **1** (4.6 mg, t_R = 30.0 min) and **2** (3.5 mg, t_R = 32.0 min). Subfraction B3 (3.7 g) was isolated by ODS using MeOH-H_2O in gradient from 10:90 to 60:40. Then, Sephadex LH-20 (isocratic elution in MeOH) and preparative HPLC (isocratic elution in MeOH–H_2O, 60%) were used to receive substances **3** (3.9 mg, t_R = 26.1 min), **4** (4.2 mg, t_R = 28.8 min) and **5** (4.8 mg, t_R = 30.4 min). Compounds **6** (4.8 mg, t_R = 33.5 min), **7** (6.3 mg, t_R = 34.8 min) and **8** (7.7 mg, t_R = 35.7 min) were separated from subfraction C (6.7 g) by ODS using MeOH-H_2O in gradient from 10:90 to 60:40. Then Sephadex LH-20 (isocratic elution in MeOH) and preparative HPLC (gradient elute in MeOH–H_2O, 70–30%) were used for further isolation. Preparative HPLC was used to separate subfraction C 3–6 (220 mg) using 71% MeOH-H_2O to obtain substances 9 (8 mg, t_R = 38.5 min) and 10 (9 mg, t_R = 39.5 min).

Furthermore, compound **4** and **5** were further isolated into the pure enantiomers **4a** (1.0 mg, t_R = 14.3 min), **4b** (1 mg, t_R = 27.7 min), **5a** (1 mg, t_R = 25.8 min) and **5b** (1 mg, t_R = 34.2 min), respectively, by chiral HPLC column using a CHIRALCEL-OJ-H (4.6 mm × 250 mm, 5 μm, n-hexane: isopropyl alcohol 90: 10, 0.8 mL/min).

Cosmochlorin F **(1)**: Amorphous colorless and white powder; UV: 210 nm, 292 nm IR (KBr): 3439, 2922, 1616, 1346 cm^{-1}; [α] $^{20}_D$ −62.1 (c 0.1, MeOH); HR-ESI-MS *m*/*z* 291.0691 $[M+H]^+$ (calcd for 291.0689, $C_{13}H_{17}{}^{35}Cl_2O_3$), *m*/*z* 293.0662 $[M+H]^+$ (calcd for 293.0660, $C_{13}H_{17}{}^{35}Cl^{37}ClO_3$); ^{1}H-NMR (400 MHz, DMSO-d_6) data listed in Table 1; ^{13}C-NMR (100 MHz, DMSO-d_6) data listed in Table 2.

Table 1. ^{1}H NMR data (400 MHz) for compounds **1, 2, 3, 4** and **5** in DMSO-d_6.

No.	δ_H (*J* in Hz)				
	1	**2**	**3**	**4**	**5**
1	6.84 s	6.96 s	6.89 s	6.92 s	6.90 s
7	-	-	-	-	-
8	5.16 dd (4.0, 8.0)	2.49 s	3.52 s	3.63 s	3.94 s
9	4.53 t (6.3)	-	3.51 s	3.6 s	-
10	1.18 d (6.3)	-	-	-	6.23 s
11	-	-	5.49 dt (1.1, 8.4)	6.25 s	-
12	-	-	4.85 s	-	-
13	-	-	1.48 s	2.22 s	-
1′	1.80 d (6.3)	-	1.45 t (7.1)	1.39 s	1.43 s
2′	-	-	1.81 s	2.24 d (0.7)	1.96 s
2, 6-OMe	3.90 d (0.9)	3.94 s	3.90 d (1.3)	3.92 d (3.38)	3.91 d (3.89)
N-CH_3	-	-	1.48	1.45	-

Cosmochlorin G **(2)**: Amorphous colorless and white powder; UV: 210 nm, 295 nm IR (KBr): 3421, 2921, 1630, 1335 cm^{-1}; HR-ESI-MS *m*/*z* 249.0081 $[M+H]^+$ (calcd for 249.0079, $C_{10}H_{11}{}^{35}Cl_2O_3$), *m*/*z* 251.0049 $[M+H]^+$ (calcd for 251.0046, $C_{10}H_{11}{}^{35}Cl^{37}ClO_3$); ^{1}H (400 MHz, DMSO-$d_6$) data listed in Table 1; ^{13}C NMR (100 MHz, DMSO-d_6) data listed in Table 2.

Cosmochlorin H **(3)**: Amorphous colorless and white powder; UV: 210 nm, 295 nm IR (KBr): 3393, 2947, 1658, 1413, 1031 cm^{-1}; HR-ESI-MS *m*/*z* 388.1196 $[M + Na]^+$ (calcd for 388.1194, $C_{16}H_{23}Na^{35}Cl_2NO_4$); ^{1}H (400 MHz, DMSO-$d_6$) data listed in Table 1; ^{13}C NMR (100 MHz, DMSO-d_6) data listed in Table 2.

Cosmochlorin I **(4)**: Amorphous colorless and white powder; UV: 210 nm, 296 nm IR (KBr): 3386, 2948, 1652, 1413, 1031 cm^{-1}; HR-ESI-MS *m*/*z* 360.3237 $[M-H]^-$ (calcd for 360.3235, $C_{16}H_{20}{}^{35}Cl_2NO_4$); ^{1}H (400 MHz, DMSO-$d_6$) data listed in Table 1; ^{13}C NMR (100 MHz, DMSO-d_6) data listed in Table 2.

Table 2. ^{13}C NMR data (100 MHz) for compounds **1, 2, 3, 4** and **5** in DMSO-d_6.

No.	δ_C				
	1	**2**	**3**	**4**	**5**
1	98.0	98.7	97.8	98.0	97.9
2, 6	154.2	154.7	154.7, 154.0	154.1, 154.6	154.6, 154.0
3, 5	111.8, 112.1	107.2	113.5, 111.6	113.2, 111.5	113.2, 111.7
4	142.7	140.7	138.2	137.8	137.8
7	129.6	199.7	-	-	61.8
8	136.8	30.8	63.1	63.2	62.5
9	63.1	-	63.4	65.1	142.2
10	23.7	-	127.0	148.3	131.2
11	-	-	137.6	124.3	200.4
12	-	-	61.6	198.3	-
13	-	-	16.7	32.0	-
1′	16.3	-	24.5	15.5	16.7
2′	-	-	21.4	16.7	20.5
2, 6-OMe	56.6	56.9	56.7	56.8	56.7

Cosmochlorin J (**5**): Amorphous colorless and white powder; UV: 210 nm, 295 nm IR (KBr): 3395, 2921, 1645, 1429, 1046 cm^{-1}; HR-ESI-MS m/z 347.0779 $[M-H]^-$ (calcd for 347.0783, $C_{15}H_{17}{}^{35}Cl_2O_5$), m/z 349.0762 $[M-H]^-$ (calcd for 249.0760, $C_{15}H_{17}{}^{35}Cl^{37}ClO_5$), m/z 351.0838 $[M-H]^-$ (calcd for 351.0840, $C_{15}H_{17}{}^{37}Cl_2O_5$); ^1H (400 MHz, DMSO-d_6) data listed in Table 1; ^{13}C NMR (100 MHz, DMSO-d_6) data listed in Table 2.

2.4. ECD Calculations

Spartan was employed to carry out the absolute configurations of substances **1** and **4**.

For further optimization, the conformational analysis was performed using the density functional theory method at the B3LYP/6-31G(d) level in the Gaussian 09 program package [23]. Time-dependent density functional theory (TDDFT) was used for the theoretical electronic circular dichroism (ECD) calculations. The parameters were selected at the B3LYP/6-31 + G(d,p) level with Boltzmann processing in MeOH using the conductor-like polarizable continuum model (CPCM). SpecDis 1.51 was used for the calculated ECD curves.

2.5. Optical Rotation Calculations

Sybyl-X 2.0 was used for conformational analyses of compound **5**. A MMFF94S force field was used with an energy cut-off of 2.5 kcal/mol [7]. A GAUSSIAN 09 program was performed at the B3LYP-D3(BJ)/6–31G* level in PCM MeOH [7]. DFT was optimized for all the conformers. To obtain the Boltzmann-weighted conformer population, the Gibbs free energy equation ($\Delta G = -RT \ln K$) was carried out. Gaussian 09 using the DFT method was performed for the optical rotation calculations at the CAM-B3LYP/6-311 + G (2d, p) level in polarizable continuum model (PCM) in MeOH solvent [7].

2.6. Cytotoxic Assay

The cytotoxicities of compounds **1—10** toward H9 (Human T lymphoid cell lines), HL-60 (Human promyelocytic acute leukemia cell lines), K562 (Human chronic myelogenous leukemia cancer cell lines), THP-1 (mononuclear macrophage cell lines) and CEM (leukemia cell lines) were assayed using the MTT method [24]. The cell lines were all bought from the Chinese Academy of Sciences Committee on Type Culture Collection Cell Bank (Shanghai, China).

2.7. Molecular Docking

The Protein Data Bank RCSB (https://www.rcsb.org/#Category-search, accessed on 11 April 2023) was used to obtain the crystal structure of ERK2 with PDB Code 6GDQ [14]. The molecular docking method was used on the basis of our former description [25]. Discovery Studio 4.3 (Accelrys Inc., San Diego, CA, USA) was used to prepare the protein

structure. For docking studies, water molecules were deleted and hydrogen atoms were appended, and the chemical structures were handled in the format of PDB. Sybyl software (Tripos, St Louis, USA) was used for the 3D structures of substances **1** and **2** by adding Gasteiger–Hückel charges. The ligand was submitted to minimize energy using the Tripos force field parameters [26]. A Molegro Virtual Docker 4.0 (Molegro ApS, Aarhus, Denmark) was put into effect by blind docking. The protein can be covered by the 3D docking grid sufficiently.

3. Results and Discussion

3.1. Structure Elucidation of Secondary Metabolites

Substance **1** was obtained as an amorphous colorless and white powder. The molecular formula of compound **1** was determined to be $C_{13}H_{17}Cl_2O_3$ based on HR-ESI-MS ($[M+H]^+$ at m/z 291.0691, calcd 291.0689, $C_{13}H_{17}Cl_2O_3$ and m/z 293.0662, calcd 293.0660, $C_{13}H_{17}{}^{35}Cl^{37}ClO_3$). In the spectrum of ^{1}H NMR (Table 1), there were feature semaphores for a phenyl ring at δ_H 6.84 (1H, s), two methoxyls at δ_H 3.90 (6H, d), two methine signals at δ_H 5.16 (1H, dd, J = 4.0, 8.0 Hz) and δ_H 4.53 (1H, t, J = 4.0 Hz), as well as two feature semaphores of methyl proton at δ_H 1.80 (3H, d) and δ_H 1.18 (3H, d, J = 4.0 Hz). The spectra of ^{13}C NMR (Table 2) and HSQC of **1** offered twelve aromatic carbons. The resonances at δ_C 98.0 (C-1), 154.1 (C-2), 154.2 (C-6), 111.8 (C-3), 112.1 (C-5) and 142.7 (C-4) were assigned similar to the carbons of Cosmochlorin D [21], which were also replaced by two methyls and two chlorines. These partial structures were further acknowledged by means of long-range correlations with the experiments of HMBC as listed in Figures 1 and 2. The correlations received from HMBC such as H-1(δ_H 6.84) to C-3 (δ_C 111.8), C-5 (δ_C 112.1) and C-2,6 (δ_C 154.1) confirmed the existence of a benzene ring. In the spectrum of H-H COSY (Figure S2-4), there had been correlations between H-1 (δ_H 6.84) and 2,6-OCH_3(δ_H 3.90 d). In the HMBC signals from H-1′ (δ_H 1.80) to C-4 (δ_C 142.7) and H-8 (δ_H 5.16) to C-4 (δ_C 142.7), C-7 (δ_C 129.6), C-9 (δ_C 63.1) and C-10 (δ_C 23.7) demonstrated that a substituent group was at the position of C-4 linking to the benzene ring, which further verified the planar construction configuration of **1** (Figure 2). The absolute configurations were further confirmed by contrasting the experimental ECD with calculated ECD by employing DFT calculations (Figure 3A). Compound **1** gave positive cotton effects at 200–220 nm and 240 nm, and anastomosed well with the calculated configuration of 9*S*. Thus, the absolute configuration of substance **1** was elucidated as 9*S* and given the name Cosmochlorin F.

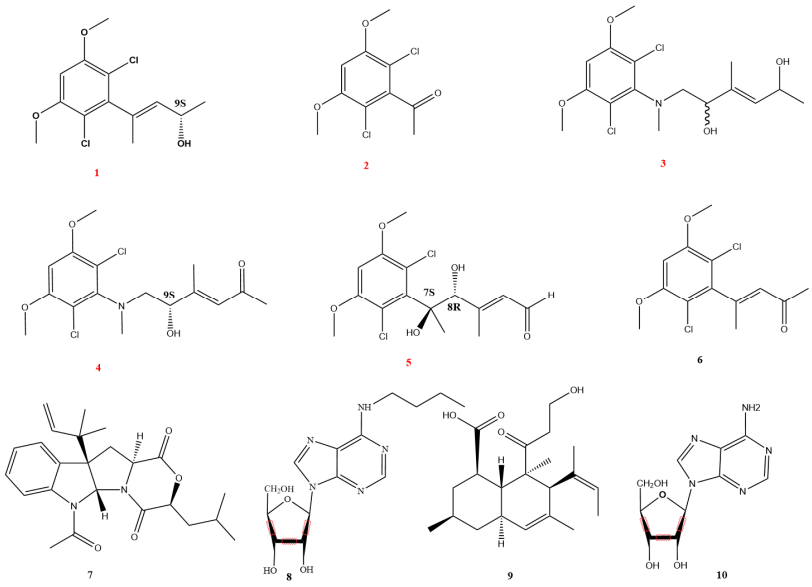

Figure 1. Metabolites **1–10** isolated from the cultivated culture of *Chaetomium* sp. SYP-F6997.

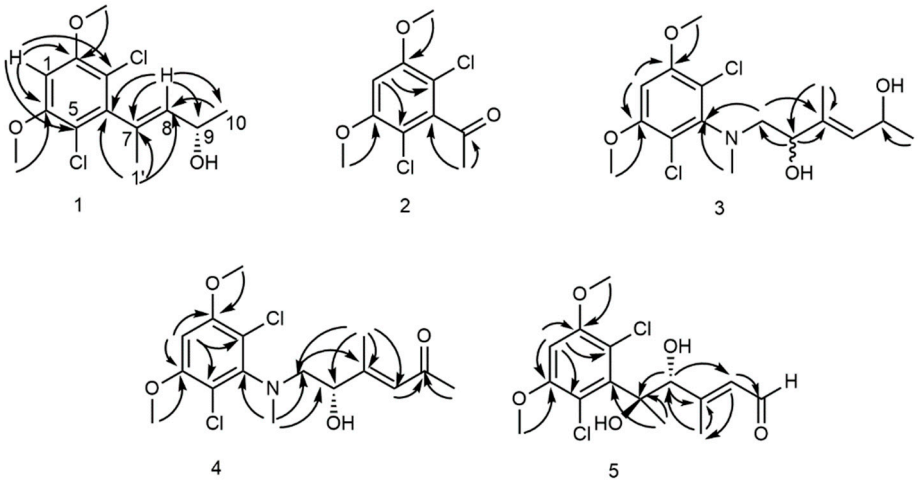

Figure 2. Key HMBC (H → C) correlations of compounds **1–5**.

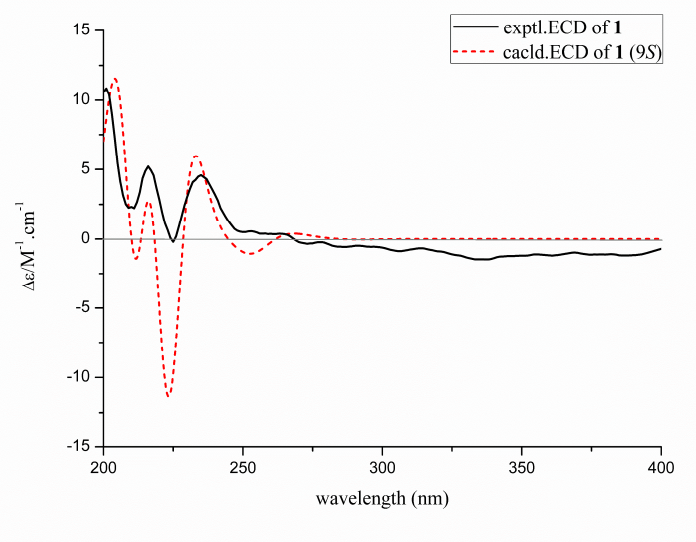

A

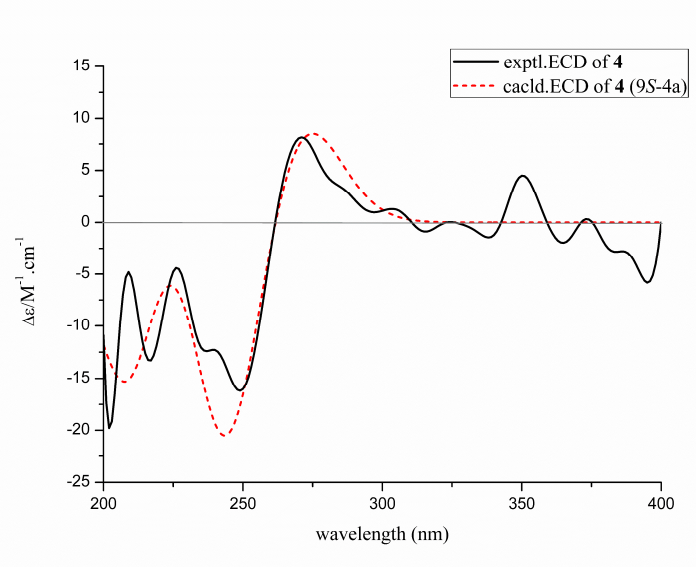

B

Figure 3. Calculated and experimental ECD spectra of compound **1** (**A**) and **4a** (**B**).

Compound **2** was acquired as an amorphous colorless and white powder. The chemical structural formula of compound **2** was $C_{10}H_{10}Cl_2O_3$, deducing from HR-ESI-MS ($[M+H]^+$ at m/z 249.0081, calcd 249.0079, $C_{13}H_{17}{}^{35}Cl_2O_3$ and m/z 251.0049, calcd 251.0046, $C_{10}H_{11}{}^{35}Cl^{37}ClO_3$). In the spectrum of ^{1}H NMR (Table 1), there were feature semaphores for a phenyl ring at δ_H 6.96 (1H, s), two methoxyls at δ_H 3.94 (6H, s) and one methyl proton signal at δ_H 2.49 (3H, s, H-8). In the spectra of ^{13}C NMR (Table 2) and HSQC (Figure S3-3), there were feature semaphores for a ketone carbonyl carbon at δ_C 199.4 (C-7) and seven aromatic carbons. The signals at δ_C 98.7 (C-1), 154.7 (C-2, 6), 107.2 (C-3, 5) and 140.7 (C-4) were assigned similar to the carbons of compound **1**, which is also replaced by two methyls and two chlorines. These partial structures were also found by HMBC experiments as listed in Figure 2. In the data of HMBC, there were signals from H-1(δ_H 6.86) to C-3,5 (δ_C 107.2), H-1 (δ_H 6.86) to C-2, 6 (δ_C 154.7) and H-2, 6-OMe (δ_H 3.94) to C-2,6 (δ_C 154.7) confirming the existence of a benzene ring. In the HMBC, there had been correlations from H-8 (δ_H 2.49) to C-7 (δ_C 199.4) and H-8 (δ_H 2.49) to C-4 (δ_C 140.7), which confirmed the side chain of compound 2. Thus, compound **2** was confirmed (Figures 1 and 2) and given the name Cosmochlorin G.

Compound **3** was acquired as an amorphous colorless and white powder. The chemical structural formula of compound 3 was $C_{16}H_{23}NaCl_2NO_4$, deducing from HR-ESI-MS ($[M+Na]^+$ at m/z 388.1196, calcd 388.1194, $C_{16}H_{23}NaCl_2NO_4$). In the spectrum of ^{1}H NMR (Table 1), there were feature semaphores for a phenyl ring at δ_H 6.89 (1H, s), an active hydrogen signal at δ_H 8.32 (1H, s), two methoxyls at δ_H 3.91 (6H, d), three methyl signals at δ_H 1.81 (3H, s), δ_H 1.48 (3H, s) and δ_H 1.45 (3H, s), one methylene signal at δ_H 3.52 (2H, s) as well as three methine signals at δ_H 5.49 (1H, d), δ_H 4.85 (1H, m) and δ_H 3.51 (1H, s). In the data of ^{13}C NMR (Table 2), there were fifteen carbons including δ_C 98.7 (C-1), 154.7 (C-2), 154.0 (C-6), 112.5 (C-3), 111.6 (C-5) and 138.2 (C-4). They were assigned similar to the carbons of Cosmochlorin D [21], which were also replaced by two methyls and two chlorines. In the spectrogram of HMBC, there were correlations (Figure 2) from H-8 (δ_H 3.52) to C-9 (δ_C 63.4), H-8 (δ_H 3.52) to C-10 (δ_C 127.0), H-9 (δ_H 3.51) to C-8 (δ_C 63.1), H-9 (δ_H 3.51) to C-10 (δ_C 127.0), H-2′ (δ_H 1.81) to C-10 (δ_C 127.0), H-2′ (δ_H 1.81) to C-9 (δ_C 63.4) and from H-13 (δ_H 1.48) to C-12 (δ_C 61.6). The HMBC cross-peaks from OCH_3 (δ_H 3.9) to C-2,6 (δ_C 154.7, 154.0) indicated the presence of two OCH_3 linking to C-2 and C-6 of the phenyl in compound **3**. The HMBC spectrum showed correlations of N-CH_3 (δ_H 1.48) with C-4 (δ_C 138.2), which indicated evidence for the nitrogen-atom connecting to the phenyl in compound **3**. The key NOESY (Figure S4-5) of compound **3** were observed between H-8 (δ_H3.94), H-1′ (δ_H1.43) and H-2′ (δ_H1.96), demonstrating that 7-CH_3/8-OH were on a trans-orientation of the substance, which further ensured the planer structure of **3** (Figure 2), which was given the name Cosmochlorin H.

Compound **4** was acquired as an amorphous colorless and white powder. The chemical structural formula of compound **4** was $C_{16}H_{21}Cl_2NO_4$, deducing from HR-ESI-MS ($[M-H]^-$ at m/z 360.3237, calcd 360.3235, $C_{16}H_{20}Cl_2NO_4$). In the spectrum of ^{1}H NMR (Table 1), there were signals of feature semaphores for a phenyl ring at δ_H 6.92 (1H, s), two methoxyl protons at δ_H 3.92 (6H, d), a vibrant hydrogen signal at δ_H 8.32 (1H, s), three methyls at δ_H 2.24 (3H, d), δ_H 2.22 (3H, s) and δ_H 1.39 (3H, s), one methine signal at δ_H 1.39 (3H, s) as well as one methylene proton at δ_H 3.63 (2H, s). In the data of ^{13}C NMR (Table 1), there were signals of sixteen carbons. The resonances at δ_C 98.0 (C-1), 154.1 (C-2), 154.6 (C-6), 113.2 (C-3), 111.5 (C-5) and 137.8 (C-4) were also assigned similar to the carbons of Cosmochlorin D [21], which were also replaced by two methoxys (δ_C 56.7 and 56.8, respectively) and two chlorines. The DEPT135° spectrum of **4** (Figure S5-3) showed methylene signals at δ_C 63.2 (C-8), methine signals at δ_C 65.1 (C-9), double bonds of carbon–carbon at δ_C 148.3 (C-10) and δ_C 124.3 (C-11), three methyl feature semaphores at δ_C 32.0 (C-13), δ_C 16.7 (C-2′) and δ_C 15.4 (C-1′). The ^{13}C NMR signals above were similar to the carbons of compound **3**, the difference being the carbonyl signals at δ_C 198.3 (C-12). In the data of HMBC (Figure 2), there were semaphores from H-2′ (δ_H 2.24) to C-10 (δ_C 148.3), H-2′ (δ_H 2.24) to C-9 (δ_C 65.1), H-2′ (δ_H 2.24) to C-8 (δ_C 63.2), H-2′ (δ_H 2.24) to C-11 (δ_C 124.3), H-8 (δ_H 3.63) to C-10

(δ_C 148.3), H-9 (δ_H 3.63) to C-10 (δ_C 148.3), H-13 (δ_H 2.22) to C-12 (δ_C 198.3), H-1′ (δ_H 1.39) to C-4 (δ_C 137.8), H-1′ (δ_H 1.39) to C-8 (δ_C 63.2), H-1′ (δ_H 1.39) to C-9 (δ_C 65.1), H-11 (δ_H 6.25) to C-9 (δ_C 65.1), H-11 (δ_H 6.25) to C-10 (δ_C 148.3) and H-11 (δ_H 6.25) to C-12 (δ_C 198.3), revealing the existence of a benzoyloxy component with a chain fragment team seated at C-4. The HMBC cross-peaks from OCH_3 (δ_H 3.92) to C-2,6 (δ_C 154.1, 154.6) indicated the presence of two OCH_3 linking to C-2 and C-6 of the phenyl in compound **4**. The HMBC spectrum also showed correlations of N-CH_3 (δ_H 1.45) with C-4 (δ_C 137.8), which indicated evidence for the nitrogen-atom connecting to the phenyl in compounds **4**. Above all, the planar construction of compound 4 was confirmed and given the name Cosmochlorin I. Further, chiral analytical HPLC (reversed-phase) was used to separate compound **4** to yield **4a** and **4b**. The spectra of experimental ECD of 4a matched well with the quantum mechanically calculated ECD spectra of 9 *S* (Figure 3B). Thus, 9*S* and 9 *R* were confirmed as the absolute configurations of substances **4a** and **4b**, respectively.

Compound **5** was acquired as an amorphous colorless and white powder. The chemical structural formula of compound 5 was $C_{15}H_{18}Cl_2O_5$, deducing from HR-ESI-MS ($[M-H]^-$ at m/z 347.0779, calcd 347.0783, $C_{15}H_{17}Cl_2O_5$ and m/z 351.0838, calcd 351.0840, $C_{15}H_{17}{}^{37}Cl_2O_5$). In the spectrum of ^{1}H NMR (Table 1), there were feature semaphores for a ring of phenyl structures at δ_H 6.90 (1H, s), two methoxyl protons at δ_H 3.91 (6H, d), one alkene proton at δ_H 6.23 (1H, s) for H-10, and two signals of methyl structures at δ_H 1.96 (3H, s, H-2′) and δ_H 1.43 (3H, s, H-1′). In the data of ^{13}C NMR (Table 2), there were signals of fifteen carbons. The resonances at δ_C 97.9 (C-1), 154.0 (C-2), 154.6 (C-6), 113.2 (C-3), 111.7 (C-5), 137.8 (C-4) and 56.7 (C-2, 6-OMe) were also assigned similar to the carbons of Cosmochlorin D [21], which were also replaced by two methoxyls and two chlorines. The DEPT135° spectrum of **5** (Figure S6-3) showed positive peaks at δ_C 62.5 (C-8), δ_C 131.2 (C-10), δ_C 16.7 (C-1′) and 20.5 (C-2′), combined with ^{13}C NMR signals at δ_C 61.8 (C-7) and δ_C 62.5 (C-8), revealing the presence of quaternary carbons and tertiary carbons with an electron-withdrawing group -OH at C-7 and C-8, respectively. In the data of HMBC, there were correlations (Figure 2) from H-8 (δ_H 3.94) to C-7 (δ_C 61.8), H-8 (δ_H 3.94) to C-9 (δ_C 142.2), H-8 (δ_H 3.94) to C-10 (δ_C 131.2), H-2′ (δ_H 1.96) to C-9 (δ_C 62.5), H-2′ (δ_H 1.96) to C-9 (δ_C 142.2), H-2′ (δ_H 1.96) to C-10 (δ_C 131.2), H-10 (δ_H 6.23) to C-9 (δ_C 142.4), H-10 (δ_H 6.23) to C-11 (δ_C 200.4), H-10 (δ_H 6.23) to C-2′ (δ_C 20.5), H-10 (δ_H 6.23) to C-8 (δ_C 62.5), H-1′ (δ_H 1.43) to C-7 (δ_C 61.8) and H-1′ (δ_H 1.43) to C-4 (δ_C 137.8), revealing an existing fragment of a benzoyloxy structure with a chain fragment group located at C-4 with C7 (C1′)-C8-C9 (C2′)-C10-C11. The key NOESY (Figure S6-6) of compound **5** were observed between H-8 (δ_H3.94), H-1′ (δ_H1.43) and H-2′ (δ_H1.96), demonstrating that 7-CH_3/8-OH were on a trans-orientation of the molecule, and so the compound was given the name Cosmochlorin J. Further, HPLC equipped with a chiral normal-phase analytical column was used for compound **5** to afford enantiomers **5a** and **5b**. However, the calculated ECD curve of **5a** and **5b** did not agree very well with their experimental ECD curves. Thus the optical rotation of **5a** (−0.0058) and **5b** (+0.0056) were tested. The optical rotation calculations of 7*S*, 8*R* (**5a,** −87.1) and 7*R*, 8*R* (**5b**, +40.4) were implemented employing a gauge-invariant atomic orbital (GIAO)-based method in the solvent of DMSO-d6. The polarizable continuum model (PCM) at the B3LYP/6-311 + G(2d, p) level was selected [23]. Thus, 7*S*, 8*R* and 7*R*, 8*R* were defined as the absolute configurations of **5a** and **5b**, respectively.

In addition, the separation of the metabolites from *Chaetomium* sp. SYP-F6997 has led to the isolation of five known substances (**6–10**), covering Cosmochlorin D (**6**) (Figure S7) [21], Javanicunines A (**7**) (Figure S8) [27], 10-butylamino-Adenosine (**8**) (Figure S9) [28], Onydecalin B (**9**) (Figure S10) [29] and Adenosine (**10**) (Figure S11) [30]. It is the first time that substances **1–10** from the genus *Chaetomium* have been reported, and the first report of compounds **1–5** and **7** from the family *Chaetomiaceae*.

The basic carbon skeletons of compounds **1–6** are similar. Thus, their possible biosynthetic pathways are proposed according to previous research results. Cosmochlorin D (**6**), known as a derivative of dichlorophenols, appertains to the polyketide group. Polyketides are groups of a large number of natural products with analogous biosynthetic pathways [31].

The compounds (**1–6**) might be derived starting from a group of acetates and extended chains by malonate reacting [32].

The molecules might be made by aldol reaction/hydroxylation/hydrolysis reactions and decarboxylation/oxidation/chlorination/alkylation reactions, which might be the speculated precursors of Cosmochlorin series compounds. The exploratory biosynthetic pathways of **1–6** are shown in Figure S12.

3.2. Activities Assay

All of the substances were tested for their cytotoxic activities using H9, HL-60, K562, THP-1 and CEM cell lines by using the method of MTT (Table 3). Compound **1** displayed good cytotoxicity against H9 and CEM with IC_{50} 7.9 and 9.0 μM, while showing moderate strength against HL-60, THP-1 and K562 with IC_{50} 13.0, 13.6 and 27.2 μM. Compound **2** showed good activities against CEM and H9 with IC_{50} 8.5 and 7.9 μM, while showing moderate strength against THP-1and HL-60, with IC_{50} 26.0 and 30.0 μM, respectively.

Table 3. Inhibition effects of fungal metabolites 1–10 [a] on the growth of tumor cells in vitro [b].

Compounds	H9	HL-60	K562	THP-1	CEM
1	7.9	13.0	27.2	13.6	9.0
2	8.5	30.0	80	26.0	7.9
3	86	93	79	72	83
4	64	87	76	70	88
5	79	94	82	74	89
6	68	73	87	89	92
7	93	87	96	82	79
8	89	>100	68	>100	81
9	>100	>100	88	>100	>100
10	>100	>100	>100	>100	>100
AraC	0.016	0.015	0.036	0.040	0.0048

[a] Results are expressed as IC_{50} values in μM. AraC were used as a positive control. [b] Key: H9, Human T lymphoid cell lines; HL-60, Human promyelocytic acute leukemia cell lines; K562, Human chronic myelogenous leukemia cancer cell lines; THP-1, mononuclear macrophage cell lines; CEM, leukemia cell lines.

3.3. Molecular Docking

Because compounds **1** and **2** possessed good antitumor effects, ERK2 (PDB ID: 6GDQ) was selected as the target for docking to further analyze a feasible antitumor mechanism with them. The results acquired are shown in Figure 4 and Table 4. The docking results showed that compounds **1** and **2** displayed high binding energies, strong H-bond interactions and hydrophobic interactions with ERK2, validating the observed antitumor activities. Compound **1** formed four conventional hydrogen bondings with the LYS55, ALA35, ARG67 and GLY169 residues of ERK2. In addition, hydrophobic bonds were observed between the TYR36 of ERK2 with compound **1**. Compound **2** displayed two conventional hydrogen bindings with TYR36 and LYS55 of ERK2 (Table 4). Thus, the extra hydrogen and hydrophobic bonds were deemed to give more strength to the integration. Based on the antitumor activities and the docking results, substances **1** and **2** might be candidates for ERK2 inhibitors.

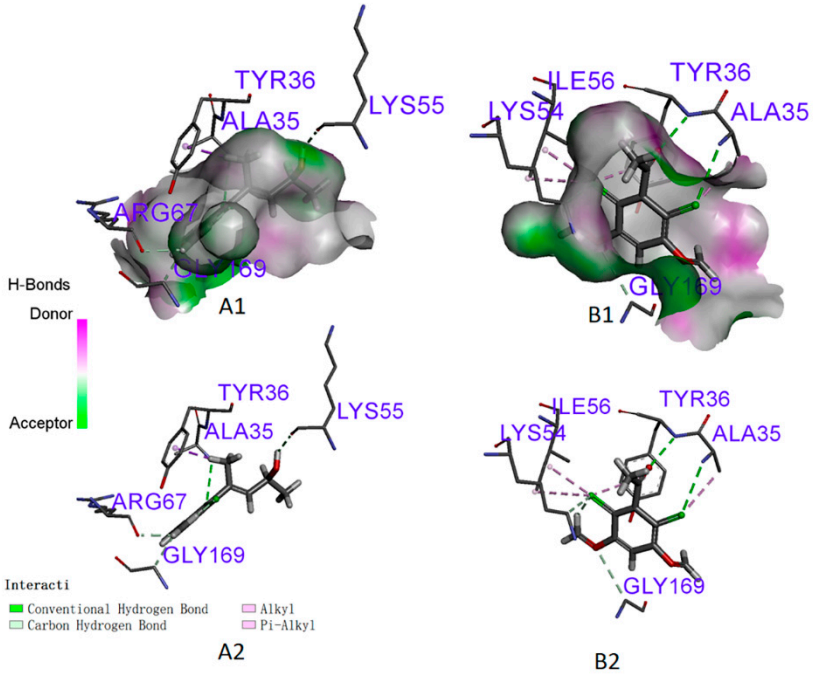

Figure 4. In silico docking simulation of compounds 1 and 2 to ERK2 (PDB ID: 6GDQ). A1: H-bond interactions between 1 and ERK2 pocket in a 3D docking model. A2: H-bond and hydrophobic interaction between 1 and ERK2. B1: H-bonds and hydrophobic interactions between 2 and ERK2 pocket in a 3D docking model. B2: H-bonds and hydrophobic interactions between 2 and ERK2.

Table 4. Binding residues involved in the formation of hydrophobic bonds and hydrogen bonds with compounds **1** and **2**.

Com.	PDB (ID)	Docking Score (Kcal/mol)	Residues	
			Conventional Hydrogen Bond	Hydrophobic Bond
1	6GDQ	−108	LYS55, ALA35, ARG67, GLY169	TYR36
2	6GDQ	−100	TYR36, LYS55	VAL39, LYS54

4. Conclusions

In conclusion, five new dichlororesorcinols, Cosmochlorin F **(1)**, Cosmochlorin G **(2)**, Cosmochlorin H **(3)**, Cosmochlorin I **(4)**, Cosmochlorin J (**5**), were separated from the endophytic fungus *Chaetomium* sp. SYP-F6997. The new substances have different cytotoxic activities against cell lines H9, HL-60, K562, THP-1 and CEM. New compounds **1** and **2** showed good antitumor activities against H9 and CEM with IC_{50} lower than 10 μM. Furthermore, molecular docking results revealed that the new compounds **1** and **2** exhibited high binding energies, strong hydrogen-bond interactions and hydrophobic interactions with ERK2, which may explain their potent antitumor activities. According to the antitumor activities and docking results, new compounds **1** and **2** might be promising antitumor lead molecules as ERK2 inhibitors.

Supplementary Materials: The following supporting information can be downloaded at: https://www.mdpi.com/article/10.3390/fermentation9060517/s1, Figure S1: Morphological images of strain SYP-F6997; Figures S2–S11: NMR Data; Figure S12: The Hypothesis of biosynthetic pathway of compounds **1**–**6**.

Author Contributions: Experimental design, Y.W., M.Z. and Y.Z.; experiment implementation, Y.W., J.C. and M.X.; data processing, J.X.; writing original draft preparation, Y.W., X.Z. and M.Z. All authors have read and agreed to the published version of the manuscript.

Funding: This research project is financially supported by the National Natural Science Foundation of China (No. 81703397), Science & Technology Fundamental Resources Investigation Program (Grant No. 2019FY100700), Liao Ning Revitalization Talents Program (XLYC1902072), Liaoning Nature Foundation (2019MS298).

Institutional Review Board Statement: Not applicable.

Informed Consent Statement: Not applicable.

Data Availability Statement: Not applicable.

Acknowledgments: We thank Yungchi Cheng for testing activities of our compounds. Department of Pharmacology, Yale University School of Medicine, New Haven, CT, United States.

Conflicts of Interest: Author Xunyong Zhou was employed by the company Zhen Cui(jiangsu) enzyme biology limited., Ltd. The remaining authors declare that the research was conducted in the absence of any commercial or financial relationships that could be construed as potential conflicts of interest.

References

1. Uzayisenga, R.; Ayeka, P.A.; Wang, Y. Anti-diabetic potential of *Panax notoginseng* saponins (PNS): A review. *Phytother. Res.* **2014**, *28*, 510–516. [CrossRef]
2. He, N.W.; Zhao, Y.; Guo, L.; Shang, J.; Yang, X.B. Antioxidant, antiproliferative, and pro-apoptotic activities of a saponin extract derived from the roots of *Panax notoginseng* (Burk.) F.H. Chen. *J. Med. Food* **2012**, *15*, 350–359. [CrossRef]
3. Wang, P.; Cui, J.; Du, X.; Yang, Q.; Jia, C.; Xiong, M.; Yang, Q.; Yu, X. *Panax notoginseng* saponins (pns) inhibits breast cancer metastasis. *J. Ethnopharmacol.* **2014**, *154*, 663–671. [CrossRef] [PubMed]
4. Zhang, H.W.; Song, Y.C.; Tan, R.X. Biology and chemistry of endophytes. *Nat. Prod. Rep.* **2006**, *23*, 753–771. [CrossRef] [PubMed]
5. Zhu, H.; Li, D.; Yan, Q.; An, Y.; Huo, X.; Zhang, T.; Zhang, M.W.C.; Xia, M.; Ma, X.; Zhang, Y. α-pyrones, secondary metabolites from fungus cephalotrichum microsporum and their bioactivities-sciencedirect. *Bioorg. Chem.* **2019**, *83*, 129–134. [CrossRef]
6. Ma, G.L.; Xi, N.G.; Wang, X.L.; Li, J.; Jin, Z.X.; Han, Y.; Su, Z.D.; Jin, J.X.; Hu, J.F. Cytotoxic secondary metabolites from the vulnerable conifer cephalotaxus oliveri and its associated endophytic fungus alternaria alternate y-4-2. *Bioorg. Chem.* **2020**, *105*, 104445. [CrossRef] [PubMed]
7. Yu, C.; Nian, Y.; Chen, H.; Liang, S.; Sun, M.; Pei, Y.; Wang, H. Pyranone Derivatives With Antitumor Activities, From the Endophytic Fungus *Phoma* sp. YN02-P-3. *Front. Chem.* **2022**, *10*, 950726. [CrossRef]
8. Xie, J.; Wu, Y.Y.; Zhang, T.Y.; Zhang, M.Y. New and bioactive natural products from an endophyte of Panax notoginseng. *RSC Adv.* **2017**, *7*, 38100–38109. [CrossRef]
9. Zhao, J.C.; Wang, Y.L.; Zhang, T.Y. Indole diterpenoids from the endophytic fungus *Drechmeria* sp. as natural antimicrobial agents. *Phytochemistry* **2018**, *148*, 21–28. [CrossRef] [PubMed]
10. Boulton, T.G.; Yancopoulos, G.D.; Gregory, J.S.; Slaughter, C.; Moomaw, C.; Hsu, J.; Cobb, M.H. An insulin-stmulated Protein kinade similar to yeast kinases involved in cell cycle control. *Science* **1990**, *249*, 64–67. [CrossRef] [PubMed]
11. Samatar, A.A. Extracellular signal-regulated kinase (ERK1 and ERK2) Inhibitors. In *Conquering RAS*; Elsevier: Amsterdam, The Netherlands, 2017; pp. 233–249. [CrossRef]
12. Savoia, P.; Fava, P.; Casoni, F.; Cremona, O. Targeting the ERK signaling pathway in melanoma. *Int. J. Mol. Sci.* **2019**, *20*, 1483. [CrossRef]
13. Marampon, F.; Ciccarelli, C.; Zani, B.M. Biological Rationale for Targeting MEK/ERK Pathways in Anti-Cancer Therapy and to Potentiate Tumour Responses to Radiation. *Int. J. Mol. Sci.* **2019**, *20*, 2530. [CrossRef]
14. Pathania, S.; Singh, P.K.; Narang, R.K.; Rawal, R.K. Identifying novel putative erk1/2 inhibitors via hybrid scaffold hopping–fbdd approach. *J. Biomol. Struct. Dyn.* **2021**, *40*, 6771–6786. [CrossRef] [PubMed]
15. Asati, V.; Mahapatra, D.K.; Bharti, S.K. PI3K/Akt/mTOR and Ras/Raf/MEK/ERK signaling pathways inhibitors as anticancer agents: Structural and pharmacological perspectives. *Eur. J. Med. Chem.* **2016**, *109*, 314–341. [CrossRef]
16. Boulton, T.G.; Nye, S.H.; Robbins, D.J.; Ip, N.Y.; Yancopoulos, G.D. ERK: A family of Protein serine/threonine kinases that are activated and tyrosine PhosPhorylated in response to insulin and NGF. *Cell* **1991**, *64*, 663–675. [CrossRef] [PubMed]
17. Lefloch, R.; Pouysségur, J.; Lenormand, P. Single and Combined Silencing of ERK1 and ERK2 Reveals Their Positive Contribution to Growth Signaling Depending on Their Expression Levels. *Mol. Cell. Biol.* **2008**, *28*, 511–527. [CrossRef]
18. Qin, J.; Xin, H.; Nickoloff, B.J. Specifically targeting erk1 or erk2 kills melanoma cells. *J. Transl. Med.* **2012**, *10*, 15. [CrossRef]
19. Shin, M.; Franks, C.E.; Hsu, K.L. Isoform-Selective Activity-Based Profiling of ERK Signaling. *J. Chem. Sci.* **2018**, *9*, 2419–2431. [CrossRef] [PubMed]
20. Fatima, N.; Muhammad, S.A.; Khan, I.; Qazi, M.A.; Shahzadi, I.; Mumtaz, A.; Hashmi, M.A.; Khan, A.K.; Ismail, T. *Chaetomium* endophytes: A repository of pharmacologically active metabolites. *Acta Physiol. Plant.* **2016**, *38*, 136. [CrossRef]

21. Shiono, Y.; Muslihah, N.I.; Suzuki, T.; Ariefta, N.R.; Anwar, C.; Nurjanto, H.H.; Aboshi, T.; Murayama, T.; Tawaraya, K.; Koseki, T.; et al. New eremophilane and dichlororesorcinol derivatives produced by endophytes isolated from ficus ampelas. *J. Antibiot.* **2017**, *70*, 1133–1137. [CrossRef]
22. Li, H.Q.; Li, X.J.; Wang, Y.L.; Zhang, Q.; Zhang, A.L.; Gao, J.M.; Zhang, X.C. Antifungal metabolites from chaetomium globosum, an endophytic fungus in ginkgo biloba. *Biochem. Syst. Ecol.* **2011**, *39*, 876–879. [CrossRef]
23. Wang, Y.X.; Zhou, L.; Lin, B.; Wang, X.B.; Huang, X.X.; Song, S.J. Anti-β-amyloid aggregation activity of enantiomeric furolactone-type lignans from Archidendron clypearia (Jack) I.C.N. *Bioorg. Chem.* **2018**, *34*, 1478–6419. [CrossRef]
24. Dai, Y.H.; Wang, A.D.; Chen, Y.L.; Xia, M.Y.; Shao, X.Y.; Liu, D.C.; Wang, D. A new indole alkaloid from the traditional chinese medicine chansu. *J. Asian Nat. Prod. Res.* **2017**, *20*, 581–585. [CrossRef] [PubMed]
25. Wu, Y.Y.; Zhang, T.Y.; Zhang, M.Y.; Cheng, J.; Zhang, Y.X. An endophytic fungi of *Ginkgo Biloba* L. produces antimicrobial metabolites as potential inhibitors of ftsz of staphylococcus aureus. *Fitoterapia* **2018**, *128*, 265–271. [CrossRef]
26. Fritsche, E.; Humm, A.; Huber, R. The ligand-induced structural changes of humanl-arginine:glycine amidinotransferase a mutational and crystallographic study. *J. Biol. Chem.* **1999**, *274*, 3026–3032. [CrossRef] [PubMed]
27. Nakadate, S.; Nozawa, K.; Horie, H.; Fujii, Y.; Nagai, M.; Komai, S.; Hosoe, T.; Kawai, K.; Yaguchi, T.; Fukushima, K. New dioxomorpholine derivatives, javanicunine a and b, from eupenicillium javanicum. *Heterocycles* **2006**, *9*, 1969–1972. [CrossRef]
28. Casati, S.; Manzocchi, A.; Ottria, R.; Ciuffreda, P. ^{1}H, ^{13}C and ^{15}N NMR assignments of adenosine derivatives with different amino substituents at C^{6}-position. Magnetic Resonance in Chemistry. *MRC Lett.* **2011**, *49*, 279–283. [CrossRef]
29. Lin, Z.; Phadke, S.; Lu, Z.; Beyhan, S.; Aziz, M.A.; Reilly, C.; Schmidt, E.W. Onydecalins, fungal polyketides with anti-histoplasma and anti-TRP activity. *J. Nat. Prod.* **2018**, *81*, 2605–2611. [CrossRef]
30. Song, M.C.; Yang, H.J.; Jeong, T.S.; Kim, K.T.; Baek, N.I. Heterocyclic compounds from *Chrysanthemum coronarium* L. and their inhibitory activity on hACAT-1, hACAT-2, and LDL-oxidation. *Arch. Pharmacal Res.* **2008**, *31*, 573–578. [CrossRef] [PubMed]
31. Shiono, Y.; Miyazaki, N.; Murayama, T.; Koseki, T.; Harizon; Katja, D.G.; Supratman, U.; Nakata, J.; Kakihara, Y.; Saeki, M.; et al. GSK-3β inhibitory activities of novel dichroloresorcinol derivatives from *Cosmospora vilior* isolated from a mangrove plant. *Phytochem. Lett.* **2016**, *18*, 122–127. [CrossRef]
32. Dewick, P.M. *Medicinal Natural Products: A Biosynthetic Approach*, 2nd ed.; John Wiley Sons Ltd.: Chichester, UK, 2002; pp. 35–96.